NATIONAL ADVISORY COMMITTEE FOR AERONAUTICS

WARTIME REPORT

ORIGINALLY ISSUED

April 1946 as
Advance Confidential Report No. 6A30

CRITICAL MACH NUMBERS OF THIN AIRFOIL SECTIONS WITH PLAIN FLAPS

By Max A. Heaslet and Otway O'M. Pardee

Ames Aeronautical Laboratory
Moffett Field, Calif.

NACA

WASHINGTON

NACA ACR No. 6A30

NATIONAL ADVISORY COMMITTEE FOR AERONAUTICS

ADVANCE CONFIDENTIAL REPORT

CRITICAL MACH NUMBERS OF THIN AIRFOIL SECTIONS WITH PLAIN FLAPS

By Max A. Heaslet and Otway O'M. Pardee

SUMMARY

The critical Mach number, as a function of lift coefficient, is determined for certain thin and moderately thick NACA low-drag airfoils. The results, which are given graphically, include calculations on the same airfoil sections with plain flaps for small flap deflections. Curves are presented indicating optimum critical conditions for the airfoils with flaps and are in a form so that they may be compared with corresponding results for zero flap deflections.

The calculations indicate that, through the use of plain flaps, an increase may be realized in the lift-coefficient range for which the critical Mach number is in the region of high values characteristic of low-drag airfoils.

INTRODUCTION

The necessity of attaining higher speeds and higher altitudes in military aircraft has focused increasing attention on the critical speeds of the airfoil sections used and, as a result of investigations concerned with the calculation of these critical speeds, certain properties of favorable airfoil sections have become known. For example, it is possible to say as a general conclusion that the type of pressure distribution associated with low-drag airfoils is one which is also favorable to the production of high-critical-speed characteristics. Moreover, as pointed out in reference 1, the thickness ratio and the camber of a wing section play an important role since the maximum value of critical Mach number decreases approximately linearly as the camber and thickness of an airfoil increases. It has therefore been almost inevitable that the airfoil sections used on recently

designed high-speed aircraft have had the type of pressure distribution associated with the low-drag airfoil and have been thinner than those used formerly.

Critical-speed curves, such as are given in reference 1, show that the low-drag airfoil has a region of lift coefficients, more or less symmetrically disposed with respect to the design lift coefficient, in which the critical Mach number variation is small, the maximum critical Mach number being achieved within the region. Outside this sector, which corresponds roughly to the lift-coefficient range for which the low-drag properties of the airfoil hold, there is a sharp decrease in the value of critical Mach number. It is obvious that a particularly advantageous situation exists if it is possible to design the wing section of an airplane so that the high-critical-speed and low-drag regions of the wing extend beyond the lift-coefficient range for normal operations. The difficulty of achieving this has already been encountered in the design of fighter aircraft where demands on the maneuverability at high speeds are great. The problem arises again in the case of long-range bombers since, on extended flights with attendant fuel consumption and with the accompanying disposal of bomb loads, the variation of lift coefficients required may be quite large. The situation is particularly acute for jet-propelled bombers since high speeds are possible of attainment over a wide range of altitude.

The theoretical results of reference 1 show quite clearly that, as the thickness of an airfoil section decreases, the maximum critical Mach number is increased but that this increase is brought about at the expense of the lift-coefficient range for the high-critical-speed region. Thus, the high-speed requirements in the design of an airplane may call for a thin wing section while other specifications may be such that the extent of lift coefficients needed at high speeds extends beyond the natural range of the airfoil. As a consequence, it becomes highly desirable to investigate any method whereby an extension of this range may be effected. One such method which could presumably be used for this purpose is the use of full-span plain flaps, for in this manner the camber may be modified and the load distribution over the airfoil disposed so that the sharp growth of the pressure peak near the nose is restricted.

In the present report, calculations have been carried out at the request of the Air Technical Service Command, U. S. Army Air Forces, to determine the critical Mach numbers,

as a function of lift coefficients for the NACA 64-, 65-, and 66-series low-drag airfoil sections with thickness-chord ratios equal to 0.06, 0.08, 0.10, and 0.12. These sections have constant ideal lift coefficients of 0.2 at which lift the load is distributed uniformly over the chords. Another portion of the theoretical calculations is devoted to the determination of the critical Mach numbers of these same airfoil sections with plain flaps, for small flap deflections, in an attempt to study the effect of such flaps on the critical Mach number curves of the airfoils.

An experimental investigation has also been carried out, under the same general research program, to determine the Mach numbers at which the force and moment characteristics of the same sections with flaps are divergent. This investigation is to be reported separately and will contain a comparison of the theoretical critical results with the experimentally evaluated divergence Mach numbers.

A complete list of symbols, as used throughout this report, may be found in the appendix.

ANALYSIS

Computation of Critical Mach Number

It is now an established convention to define the critical Mach number of a body as the Mach number of the free stream for which, at some point on the surface of the body, the fluid first reaches a velocity equal to the local velocity of sound. In an analogous manner the critical compressibility speed is defined as the free-stream speed corresponding to that at which the critical Mach number is attained. Experimental evidence, obtained from the study of airfoil sections, indicates that compression shocks are formed locally on an airfoil surface soon after, if not coincidental with, the attainment of Mach numbers corresponding to the critical speed. This shock, however, is not well defined and, so far as can be observed, no strongly developed shock front exists until the free-stream Mach number has risen somewhat above its critical value. It thus seems quite reasonable to assume, and this has been further substantiated by experiment, that for airfoils of limited thickness the critical Mach number furnishes a conservative approximation, for the designer, for the occurrence of the flow breakdown which is associated with super-critical speeds and

[redacted]

produces the sudden changes in the airfoil characteristics that are, in general, inimical to good airplane control and performance.

The critical Mach numbers in this report are calculated in the manner used in reference 1. Under the assumption that the flow is isentropic, the critical pressure coefficient is given by the relation

$$\frac{p_{cr} - p_o}{q_o} = \frac{2}{\gamma M_{cr}^2}\left[\left(\frac{2}{\gamma+1} + \frac{\gamma-1}{\gamma+1} M_{cr}^2\right)^{\frac{\gamma}{\gamma-1}} - 1\right] \qquad (1)$$

where

p_o static pressure in the free stream

p_{cr} pressure corresponding to sonic velocity at M_{cr} and occurring at minimum pressure point

V_o velocity of the free stream

a_o velocity of sound in the free stream

M_{cr} critical Mach number, equal to V_o/a_o at critical conditions

γ ratio of specific heats ($c_p/c_v = 1.4$)

ρ_o density of the fluid in the free stream

q_o dynamic pressure $\left(\frac{1}{2}\rho_o V_o^2\right)$

In order that M_{cr} be related to the low-speed pressure coefficient $P_{M=0} = \left(\frac{p-p_o}{q_o}\right)_{M=0}$ it is necessary to express the left-hand side of equation (1) in terms of $P_{M=0}$ and to this end the Kármán-Tsien formula (reference 2) has been used. Equating this result, evaluated at the critical value of M, to the right-hand side of equation (1), gives the requisite expression

[redacted]

$$\frac{2}{\gamma M_{cr}^2}\left[\left(\frac{2}{\gamma+1}+\frac{\gamma-1}{\gamma-1}M_{cr}^2\right)^{\frac{\gamma}{\gamma-1}}-1\right]=\frac{P_{M=0}}{\sqrt{1-M_{cr}^2}+\frac{M_{cr}^2}{1+\sqrt{1-M_{cr}^2}}\frac{P_{M=0}}{2}} \qquad (2)$$

For an airfoil, or an airfoil with flap, if it is possible to determine the pressure distribution for a given low-speed lift coefficient, then the critical Mach number of the airfoil can be found by means of equation (2) together with the value of pressure coefficient at the minimum pressure point. As a result of such calculations, the critical Mach number of an airfoil is found as a function of the low-speed section lift coefficient, $c_{l_{M=0}}$. For design, however, it is highly desirable to know the actual lift coefficient c_{l_M} corresponding to the Mach number of flight. In reference 3, Glauert has developed the approximation

$$c_{l_M}=\frac{c_{l_{M=0}}}{\sqrt{1-M^2}}$$

which does relate the low- and high-speed lift coefficients, and in this report the Glauert correction has been applied. Experimental observations show that the accuracy of this correction is good for Mach numbers up through critical values.

Calculation of Pressure Distributions for Airfoils with Flaps

The theoretical calculation of airfoil pressure distributions has been outlined in reference 4, and in this reference tabular data are given whereby the pressure distributions may be calculated immediately for all standard NACA airfoil sections with various types of camber lines. The velocity distribution over the airfoil is considered, in conformity with present theory, to be formed from three separate and independent parts:

1. That part of the velocity distribution associated with the basic thickness form set at zero angle of attack

[redacted]

2. That part of the distribution associated with the design load of the camber line

3. That part of the distribution associated with the additional load distribution and related to the angle of attack of the airfoil

As a result of this theory it is possible to express the pressure coefficient $P_{M=0}$ in the form

$$P_{M=0} = 1 - \left(\frac{v}{V_o} \pm \frac{\Delta u}{V_o} \pm \frac{\Delta v_a}{V_o} \right)^2 \qquad (3)$$

where $\frac{v}{V_o}$, $\frac{\Delta u}{V_o}$, and $\frac{\Delta v_a}{V_o}$ are velocity ratios corresponding respectively to parts 1, 2, and 3. This method has been used throughout the present report for airfoils with and without flaps, and the airfoil data in reference 4 have been used in all cases.

For an airfoil with plain flap it is necessary to find the effect of the flap on the values of $\frac{\Delta u}{V_o}$ and $\frac{\Delta v_a}{V_o}$, and this can be best achieved by first calculating the change in the load distribution over the airfoil which is brought about by the flap deflection. In reference 5 this problem has been treated in a semiempirical fashion for the case of conventional airfoil sections, but the theory is not immediately applicable to low-drag airfoils and, for this reason, a different approach is made modeled on the work of Glauert in reference 6 and Allen in reference 7.

It is an accepted practice to divide the chordwise lift distribution P of an airfoil into two parts: (a) the so-called "basic" lift distribution P_b, which depends on camber-line shape and is independent of the angle of attack; and (b) the additional lift distribution P_a, which is variable with angle of attack and in form is independent of the camber-line shape. When the flap on an airfoil is deflected, the change in lift distribution is called the incremental lift distribution P_δ, and the two component parts are respectively, incremental basic distribution $P_{b\delta}$, and incremental additional distribution $P_{a\delta}$. It can be shown that the

[redacted]

incremental additional distribution due to the deflection of the flap is identical in form with the additional distribution for the airfoil with flaps neutral. The incremental basic distribution must be evaluated, however, from a knowledge of the airfoil section, the nature of the flap, and the flap deflection. The determination of this variation is therefore undertaken in the following paragraphs.

In conformity with the assumptions usually made in thin-airfoil theory, the airfoil is replaced by its mean camber line. Figure 1 shows the assumed camber line distribution produced by the deflection of the flap, the hinge point of the flap lying between x_1 and x_2, AF approximating the chord-line of the airfoil. If x is measured from point A along AF and y is measured from A along a line normal to AF, then in the figure

AB is linear with equation $y=0$ for $0 \leq x \leq x_1$

BC is parabolic with equation $y = ax^2+bx+d$ for $x_1 \leq x \leq x_2$

CD is linear with equation $y-y_2 = -\tan \delta \, (x-x_2)$ for $x_2 \leq x \leq c$

where a, b, and d are arbitrary coefficients and δ is the angle the flap is deflected. The parabolic section is to extend over a very small portion of the camber line, the extent of this section being determined later, and is introduced to avoid the sharp break in slope which theoretically would exist and the subsequent requirement of a singularity in the velocity and lift distribution at the hinge point. This small portion between B and C may be thought of as a fairing of the camber line at the point of the sharp break and is consistent not only with the existence of a boundary layer on the surface of the airfoil, for the layer has a tendency to iron out such abrupt irregularities, but also with the geometry of the median line between the upper and lower surfaces of the airfoil.

If the transformation

$$x = \frac{1}{2}c\,(1 - \cos\theta)$$

is introduced, the expressions for the slopes of the three sections may be written in the forms

$$\begin{aligned}
\text{AB:}\quad & \frac{dy}{dx} = 0 \quad \text{for} \quad 0 \leq \theta \leq \theta_1 \\
\text{BC:}\quad & \frac{dy}{dx} = 2ax + b \quad \text{for} \quad x_1 \leq x \leq x_2 \\
& \quad = G\cos\theta + H \quad \text{for} \quad \theta_1 \leq \theta \leq \theta_2 \\
\text{CD:}\quad & \frac{dy}{dx} = -\tan\delta \\
& \quad = -\lambda \quad \text{for} \quad \theta_2 \leq \theta \leq \pi
\end{aligned} \tag{4}$$

where G, H, and λ, are introduced for simplicity and are defined by the above equations.

Reference 7 establishes the relationship

$$\left(\frac{{}_oP_b}{4}\right)_o = \frac{1}{2\pi}\int_o^\pi \frac{dy}{dx}\left(\cot\frac{\theta+\theta_o}{2} - \cot\frac{\theta-\theta_o}{2}\right)d\theta \tag{5}$$

where

$\left(\frac{{}_oP_b}{4}\right)_o$ basic distribution for infinitesimally thin airfoil at chordwise station corresponding to $\theta = \theta_o$

θ variable of integration

θ_o value of θ at an arbitrary fixed point

$\frac{dy}{dx}$ slope of camber line

It is obvious that this expression can be used in conjunction with the slopes given in equations (4) to determine the incremental basic distribution due to the flap deflection.

The integration of the integral is straightforward and the final result is

$$\left(\frac{c^{P_{b\delta}}}{4}\right)_o = \frac{G}{\pi}(\theta_2 - \theta_1) \sin\theta_o + \frac{\lambda}{\pi} \ln\left|\frac{\sin\frac{1}{2}(\theta_2+\theta_o)}{\sin\frac{1}{2}(\theta_o-\theta_2)}\right| - \frac{1}{\pi}(G\cos\theta_o + H) \ln\left|\frac{\sin\frac{1}{2}(\theta_2-\theta_o)\sin\frac{1}{2}(\theta_1+\theta_o)}{\sin\frac{1}{2}(\theta_1-\theta_o)\sin\frac{1}{2}(\theta_2+\theta_o)}\right| \quad (6)$$

For a given flap deflection of δ degrees the value of λ is known and it merely remains to fix the coefficients G and H and determine θ_1 and θ_2 so that the theoretical incremental basic distribution is consistent with experiment. Impose now the condition that at $x = x_1$ $(\theta=\theta_1)$ the parabola has zero slope and a radius of curvature equal to r. This requires that

$$G = \frac{c}{2r} \quad \text{and} \quad H = -\frac{c}{2r}\cos\theta_1.$$

Moreover, at $x = x_2$ $(\theta = \theta_2)$ the slope of the parabola must equal $-\lambda$, thus

$$\frac{c}{2r}(\cos\theta_2 - \cos\theta_1) = -\lambda$$

and if $\frac{r}{c}$, λ, and θ_1 are known, it is possible to find θ_2. Letting the hinge point of the flap be at $\frac{\theta_1+\theta_2}{2}$, the parabola can be oriented so that the values of θ at its end points are symmetrically disposed with respect to θ at the hinge point and for small flap deflections θ_1 and θ_2 can be found.

Using equation (6) and the derived values of the various parameters, a comparison was made between calculated values of incremental basic distribution and available experimental data for small flap deflections. It was found that when r was set equal to the thickness of the airfoil at the hinge point the agreement was quite good over the entire airfoil surface and that at the hinge point, where maximum values of $P_{b\delta}$ are attained, the results were reasonably accurate

[redacted]

to justify the use of the theory to calculate critical Mach numbers.

By the methods of reference 7 it follows that

$$c_{l_{b\delta}} = 2\lambda \sin \theta_2 + G(\theta_2-\theta_1)+ \frac{G}{2}(\sin 2\theta_2 - \sin 2\theta_1) + 2H(\sin \theta_2 - \sin \theta_1) \quad (7)$$

and

$$c_{l_{a\delta}} = 2\lambda(\pi-\theta_2) -2H(\theta_2-\theta_1) -2G(\sin \theta_2 - \sin \theta_1) \quad (8)$$

where

$c_{l_{b\delta}}$ incremental basic lift coefficient

$c_{l_{a\delta}}$ incremental additional lift coefficient

Since $\theta_2-\theta_1$ is small, for small deflections of the flap, it is possible to approximate equations (7) and (8) by simpler expressions and this was done in the calculations. Under the same assumption, the peak point of the incremental basic lift distribution is at the hinge point and can be approximated quickly.

The relation between the velocity distribution and the chordwise lift distribution over the airfoil has been given by Allen (reference 8) in the form

$$\left(\frac{v}{V_\bullet}\right)_U = \sqrt{1-P_f} + \frac{\frac{1}{4}P}{\sqrt{1-P_f}} \quad (9)$$

and

$$\left(\frac{v}{V_\bullet}\right)_L = \sqrt{1-P_f} - \frac{\frac{1}{4}P}{\sqrt{1-P_f}} \quad (10)$$

where

$\left(\frac{v}{V_o}\right)_U$ velocity over upper surface of airfoil

$\left(\frac{v}{V_o}\right)_L$ velocity over lower surface of airfoil

P_f pressure distribution over base profile

P load distribution over airfoil

Since the contribution of the flap deflection to P has been calculated, the effect on the velocity distribution can be determined. Substitution in equation (3) will give the low-speed pressure coefficient at any point along the airfoil; and, from the minimum pressure, the critical speed of the section is determinable. In calculating the contribution of the incremental basic lift distribution to the velocity on the surface of the airfoil, it is well to bear in mind that the expression for ${}_oP_{b\delta}$ given in equation (6) was derived under the assumptions of thin airfoil theory. In reference 7 it has been pointed out that to a first order of approximation

$$P_{b\delta} = \sqrt{1-P_f}\ {}_oP_{b\delta}$$

Hence, it follows that the incremental velocity associated with this portion of the lift distribution is given by $\frac{1}{4}{}_oP_{b\delta}$. The final form of equation (3) may therefore be written as

$$P_{M=0} = 1 - \left(\frac{v}{V_o} \pm \frac{\Delta u}{V_o} \pm \frac{\Delta v_a}{V_o} \pm \frac{1}{4}\,{}_oP_{b\delta}\right)^2$$

where $\frac{\Delta u}{V_o}$ is determined from the design load of the basic camber line and $\frac{1}{4}P_{b\delta}$ is a function of the flap-chord ratio and the deflection angle of the flap.

DISCUSSION OF RESULTS

In figure 2 are shewn the critical curves of a typical airfoil section (NACA 65_1-210) for various flap deflections, both positive and negative.

It is to be observed that each critical curve is composed of three distinct parts: a substantially flat top and two steep sides. These three portions correspond to three different conditions on the airfoil determining the minimum pressure peak.

The thin airfoils considered are characterized by having large additional velocities near the nose and but a moderate rise in the basic velocity distribution approaching the maximum-velocity point. The combination results in a velocity distribution which is double-peaked for lift coefficients differing more than a small amount from the design lift. The velocity peak at the nose appears suddenly, the after velocity peak still remaining; there is no continuous transition. For a certain range of lift coefficient about the design lift the forward velocity peak is less than the rear one; for this range the critical Mach number is determined by the velocities near the maximum-velocity point of the base profile modified by the small additional velocities for this region. This latter velocity peak will be termed the midpeak velocity to distinguish it from velocity peaks which appear at hinge points on flapped airfoils to be mentioned later. This range of lift coefficient corresponds to the top of the critical curve. The small additional velocities produce a near linear change in Mach number with lift coefficient, giving to the top a slight slope as shown in figure 2.

At some lift coefficient, the velocity at the forward pressure peak becomes equal to the velocity at the midpressure peak; then for large increments of lift from the design lift, the peak velocity at the nose is the maximum and changes rapidly with change in lift coefficient due to the large additional velocities. The result is that the critical Mach number falls rapidly with increasing increment in lift coefficient. The lift coefficient for which the velocities at the nose and midpressure peaks are equal is the point of intersection of the top and the side; it is the point at which the absolute maximum velocity jumps from a position aft on the airfoil section to a point in the immediate vicinity of the nose and will be denoted as the "declination

[redacted]

point" on the critical curve. There are two such declination points, for positive and negative lift increments. For positive lift increments the velocity peak at the nose appears on the upper surface; for negative lift increments it appears on the lower surface.

Since airfoils with flaps are equivalent to the original airfoil with modified camber, the effect is to change the basic velocity distribution while leaving the additional velocity distribution the same. The critical curve, then, for the flapped airfoil is very similar to the unflapped but shifted as a whole by $c_{l_{b\delta}}$. The steep sides are practically parallel, for the incremental basic velocity at the nose is negligible. The only appreciable change occurs in the top and the declination points.

For flap deflections small enough that the velocity peak at the hinge point is less than the midpeak velocity, the top of the critical curve will have essentially the same slope, since the airfoil has the same additional velocities, but is shifted up or down depending upon whether there is a negative or positive flap deflection. The increment of lift coefficient between the upper and lower declination points will consequently vary.

For flap deflections large enough that the pressure peak at the hinge point is greater than the midpeak pressure, the top of the critical curve has a lesser slope than before, the additional velocities at the hinge point being less. It is to be noted that for negative flap deflections the peak velocity at the hinge point appears on the lower surface where the additional velocity increment with lift coefficient is negative; consequently, the top of the critical curve has a reversed slope to that of the unflapped and positively flapped airfoils. This is clearly shown in figure 2.

The locus of the upper and lower critical Mach number declination points together with the top of the critical curve form what may be termed an "optimum critical curve." All points on this curve correspond to flap deflections for which, at a given lift coefficient, the airfoil section achieves the maximum possible critical Mach number, as can be seen in figure 2.

The extension of the region of high critical Mach number by means of flaps is done in two parts. The first, where the hinge pressure peak is less than the midpeak pressure, is a near linear extension of the original curve. In this region

[redacted]

a reasonable gain in lift coefficient is realized without too much sacrifice in the critical Mach number. In the second part, after the break, the hinge peak predominates; the sacrifice in critical Mach number for increased lift is correspondingly greater.

In figure 3 are shown the optimum critical curves for the NACA 64-, 65-, and 66-series of airfoils having thickness-chord ratios of 0.06, 0.08, 0.10, and 0.12 with 0.10c, 0.20c, and 0.30c plain flaps. The critical curves of the original airfoils without flaps ($\delta=0$) are in each instance shown as dotted lines. The rest of the critical curves for other flap deflections are not shown, as was done in figure 2, but rather only the locus of the declination points. These loci, as noted previously, form optimum critical curves for the given airfoils with flaps. Each of the curves in figure 3 has a form directly analogous to the optimum curve of figure 2, having the typical extension, for small flap deflections, of the high-critical-speed lift-coefficient range.

There are two predominate variations to consider: section thickness and airfoil family. By family, reference is made to the position of the velocity peak on the base profile. The curves show a general trend to higher critical Mach numbers and smaller lift-coefficient ranges for the thinner sections. The extension of the lift-coefficient range by means of flaps shows this same tendency though to a lesser degree. The decrease in the extension of the lift-coefficient range for the thinner sections is the result of higher velocity peaks at the hinge point, together with a smaller variation in velocity along the base profile so that the break in the curve occurs sooner. The larger peak velocities for the thin sections are due to the fact that the value of the peak velocity varies inversely as the section thickness at the hinge point.

The additional velocity distributions of all the 6-series airfoils considered are substantially the same over the rearward 60 percent of the chord. For this reason, all the slopes of the tops of the critical curves in any given airfoil family are essentially the same (cf. fig. 3(a) to 3(d)). The slope for different airfoil families will be different as indicated, (cf. fig. 3(d), 3(h), 3(l)) the slope decreasing for a rearward movement of the maximum velocity point on the base profile.

For the different families a rearward movement of the maximum velocity peak is indicative of three changes in

section characteristics: a lower maximum velocity and flatter profile velocity, greater additional velocities at the nose, and a thicker section at the hinge point giving lower velocity peaks there. Thus, a rearward movement in pressure peak results in slightly higher critical speeds with, however, a smaller range of lift coefficient in the high critical region together with a smaller extension of this range by the flaps.

The extension of the critical curve of an airfoil by means of flaps will vary with the flap-chord ratio, the different optimum critical curves being, however, quite similar. A study of the curves given in figure 3 indicates that, of the flaps considered, the 0.20c gives the best over-all results.

Experiments carried out in the Ames 1- by $3\frac{1}{2}$-foot high-speed tunnel, on airfoils equipped with orifices for the determination of pressure distributions, have given some insight into the validity of theoretical calculations of critical Mach numbers. The sections considered had thickness-chord ratios equal to 0.12 and 0.15, the results being compared with those given in reference 1. It was found that, throughout the high portion of the critical-speed curves for the low-drag airfoils, excellent agreement was obtained except that the points of declination of the curves were at lift coefficients somewhat beyond those predicted, especially for the case in which the peak pressure point was forward on the upper surface. The source of this discrepancy is probably twofold: some error exists in the estimation of the true lift coefficient, and the Kármán-Tsien correction formula is erroneous in the immediate vicinity of the nose. It is possible to derive a modification of the Glauert correction for lift, by means of the Kármán-Tsien pressure formula, and the change brought about in lift coefficient can be shown to be in the right direction to agree with experiment. This change, however, is small and somewhat laborious to apply and therefore was not used. That errors in predicted pressures should exist near the nose of an airfoil follows from the fact that the Kármán-Tsien formula is postulated on the use of a pressure-density relation which holds for conditions not differing greatly from those in the free stream. Near the nose, in the vicinity of the stagnation point, some discrepancy would be expected to occur, and this is confirmed by the experimental pressure distributions.

Considerations of theory and experimental results both indicate that the theoretical results are conservative. It is to be expected, however, that, for airfoils with flaps,

[redacted]

the predicted extensions of the curves should be of the right order of magnitude.

CONCLUDING REMARKS

Theoretical calculations show that the use of plain flaps on airfoil sections such as are considered in the present report will serve to increase appreciably the range of the high-critical Mach number region characteristic of low-drag airfoils. It is to be expected, judging from what experimental evidence is available, that the results will underestimate the extent of the critical curve lying between the declination points but the predicted extension, in this portion of the curve, should be of the right order of magnitude.

Ames Aeronautical Laboratory,
National Advisory Committee for Aeronautics,
Moffett Field, Calif.

REFERENCES

1. Heaslet, Max A.: Critical Mach Numbers of Various Airfoil Sections. NACA ACR No. 4G18, 1944.

2. von Kármán, Th.: Compressibility Effects in Aerodynamics. Jour. Aero. Sci., vol. 8, no. 9, July 1941, pp. 337-356.

3. Glauert, H.: The Effect of Compressibility on the Lift of an Aerofoil. R. & M. No. 1135, British A.R.C., 1927.

4. Abbott, Ira H., von Doenhoff, Albert E., and Stivers, Louis S., Jr.: Summary of Airfoil Data. NACA ACR No. L5C05, 1945.

5. Allen, H. Julian: Calculation of the Chordwise Load Distribution over Airfoil Sections with Plain, Split, or Serially Hinged Trailing-Edge Flaps. NACA Rep. No. 634, 1938.

6. Glauert, H.: Theoretical Relationships for an Aerofoil with Hinged Flap. R. & M. No. 1095, British A.R.C., 1927.

[redacted]

7. Allen, H. Julian: General Theory of Airfoil Sections Having Arbitrary Shape or Pressure Distribution. NACA ACR No. 3G29, 1943.

8. Allen, H. Julian: A Simplified Method for the Calculation of Airfoil Pressure Distribution. NACA TN No. 708, 1939.

APPENDIX

List of Symbols

a_o velocity of sound in the free stream

c chord length of airfoil

c_{l_M} section lift coefficient

$c_{l_{M=0}}$ low-speed section lift coefficient

$c_{l_{a\delta}}$ incremental additional lift coefficient

$c_{l_{b\delta}}$ incremental basic lift coefficient

M Mach number (velocity divided by velocity of sound)

P_M pressure coefficient $\left(\frac{p-p_o}{q_o}\right)$

$P_{M=0}$ pressure coefficient under low-speed conditions

P_f pressure-coefficient distribution over base profile

P chordwise lift distribution (difference between pressure coefficients on upper and lower surface of airfoil)

P_a chordwise lift distribution produced by additional load distribution

P_b chordwise lift distribution produced by basic camber-line loading

P_δ incremental load distribution produced by flap deflection

$P_{a\delta}$ incremental additional load distribution produced by flap delfection

[redacted]

$P_{b\delta}$ incremental basic load distribution produced by flap deflection

$_oP_b$ basic load distribution for infinitesimally thin airfoil

$_oP_{b\delta}$ incremental basic load distribution for infinitesimally thin airfoil

p static pressure

q dynamic pressure $\left(\frac{1}{2}\rho V^2\right)$

r radius of curvature

Δu increment of local velocity produced by basic lift distribution on airfoil

v local velocity

Δv_a increment of local velocity produced by additional lift distribution on airfoil

V_o velocity of the free stream

x distance along chord measured from leading edge of airfoil

y ordinate of camber line measured from chord line

γ ratio of specific heats $(c_p/c_v = 1.4)$

δ angle of flap deflection

θ variable defined by equation $2x = c(1 - \cos\theta)$

λ tangent of angle δ

ρ density

Subscripts

o free-stream conditions

cr critical conditions

L lower surface of the airfoil

U upper surface of the airfoil

[redacted]

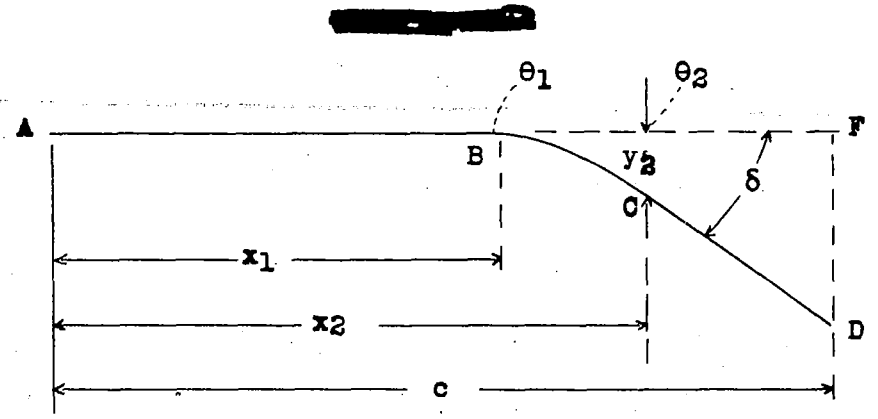

Figure 1.- Equivalent camber line for airfoil with plain flap.

NATIONAL ADVISORY COMMITTEE
FOR AERONAUTICS

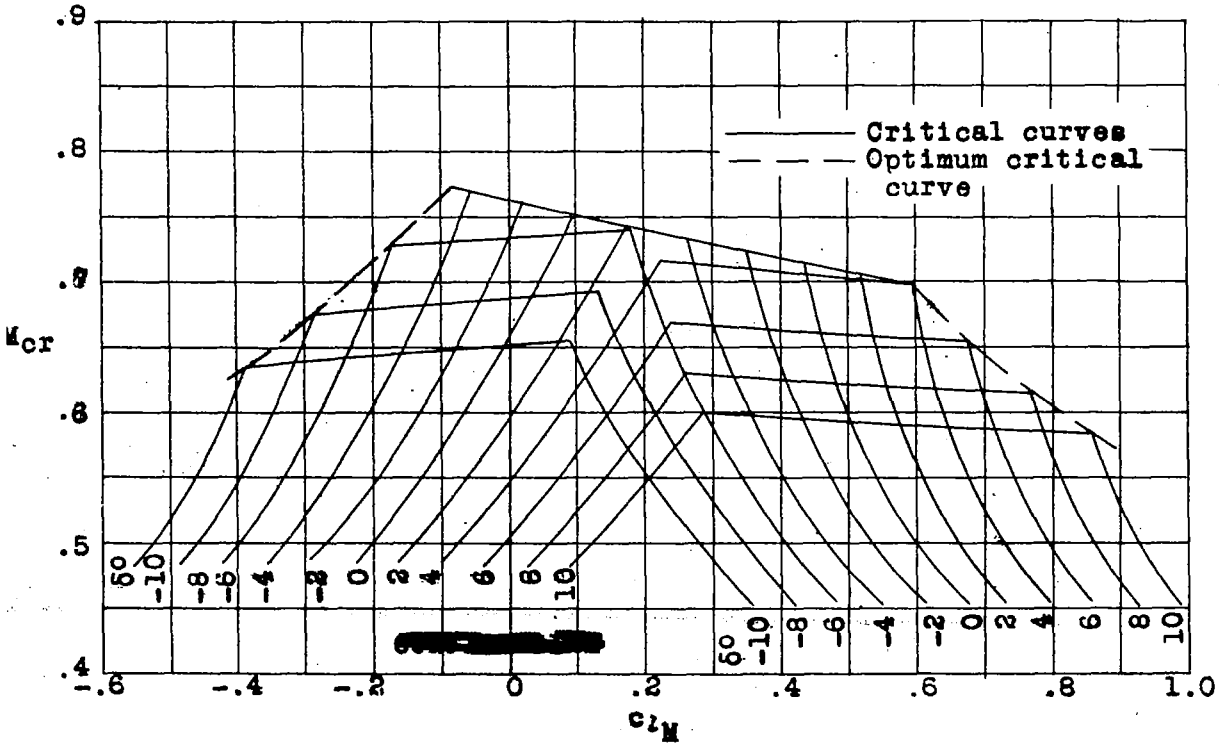

Figure 2.- Critical Mach number M_{cr} variation with high-speed lift coefficient c_{l_M} for various flap deflections δ NACA 65_1-210 airfoil section, .20c plain flap.

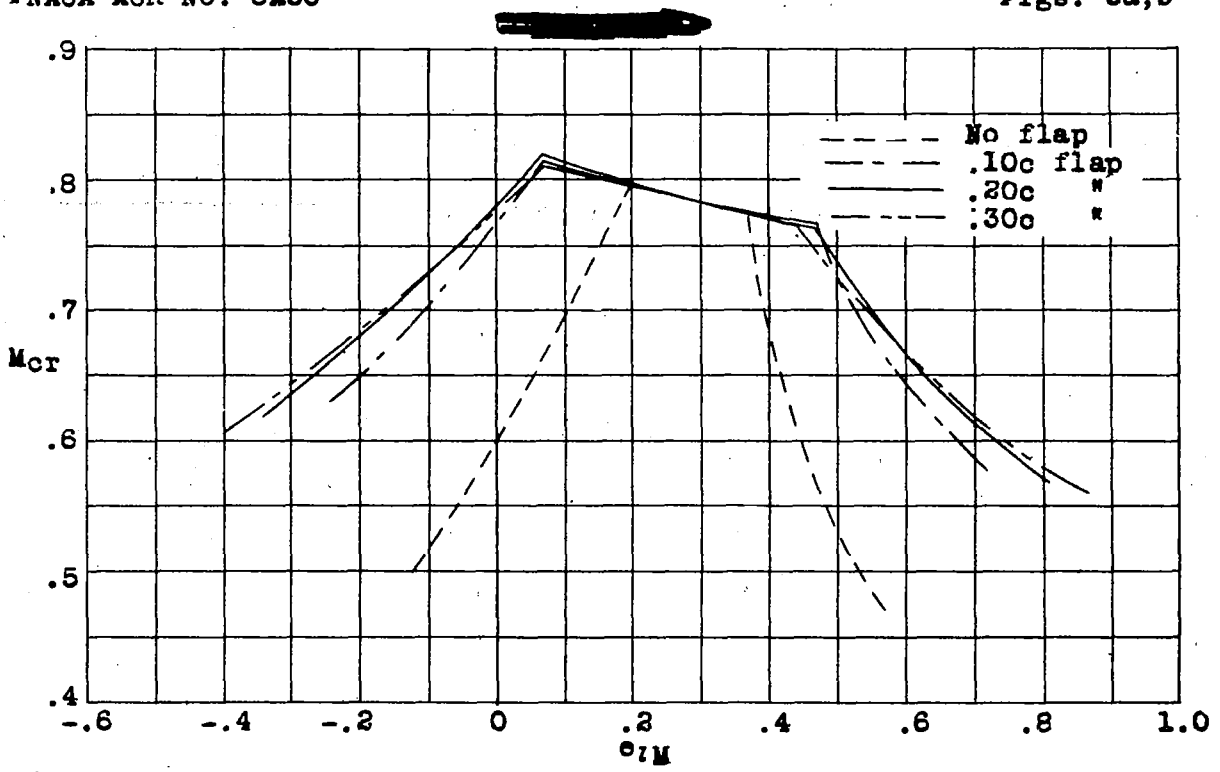

Figure 3.- Optimum critical Mach number M_{cr} variation with high-speed section lift coefficient c_{l_M} for .10c, .20c and .30c plain flaps. (a) NACA 64_1-206 airfoil section.

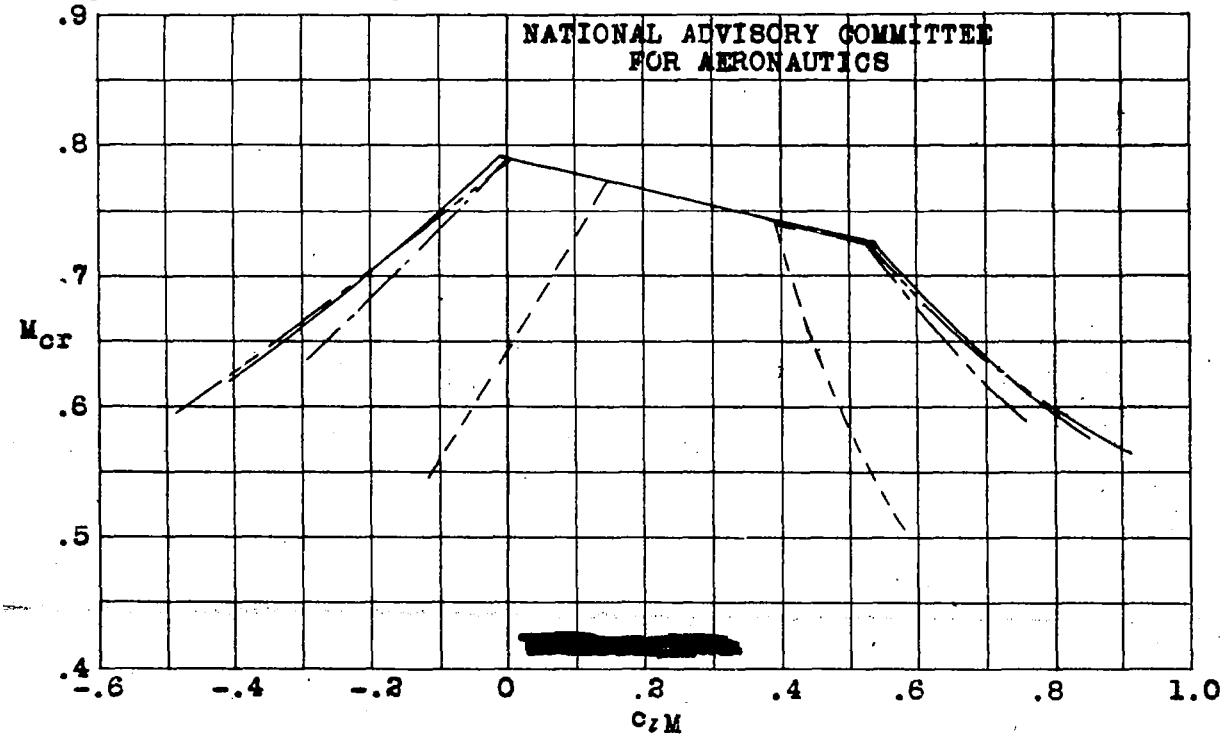

(b) NACA 64_1-208 airfoil section.

Figure 3.- Continued.

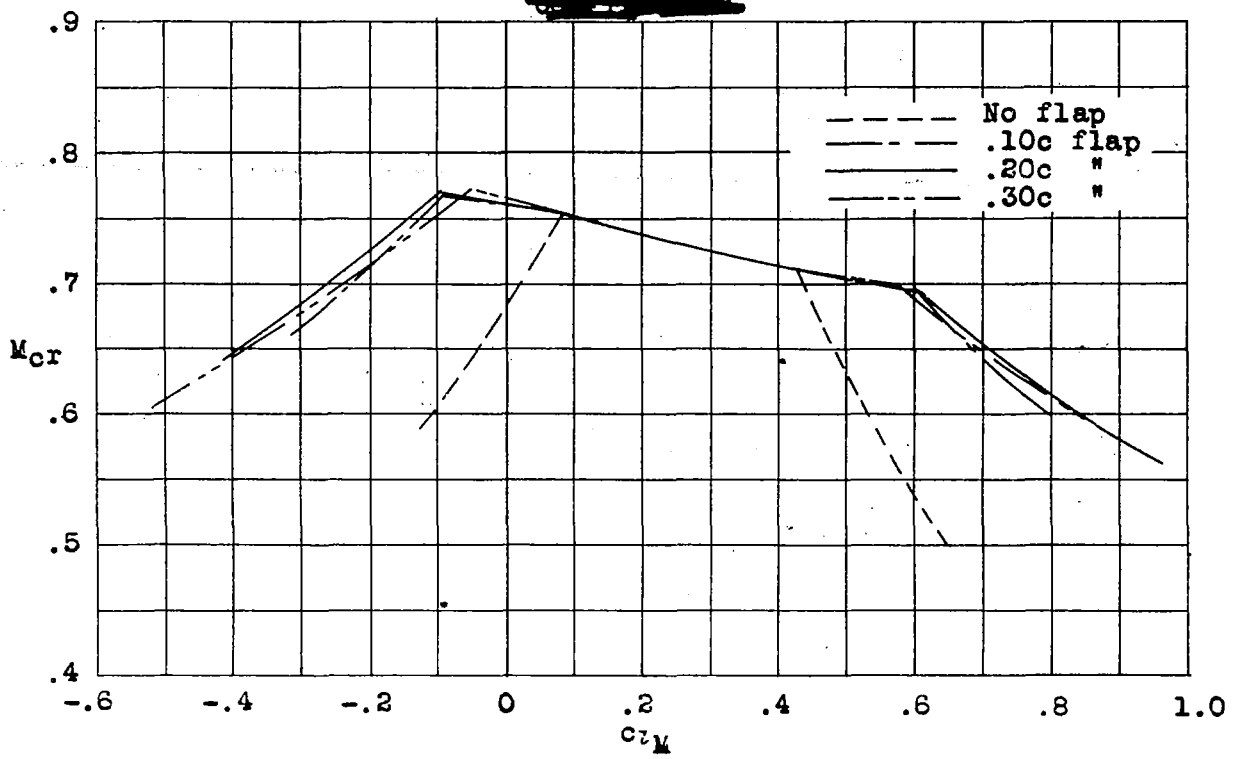

(c) NACA 64_1-210 airfoil section.
Figure 3.- Continued.

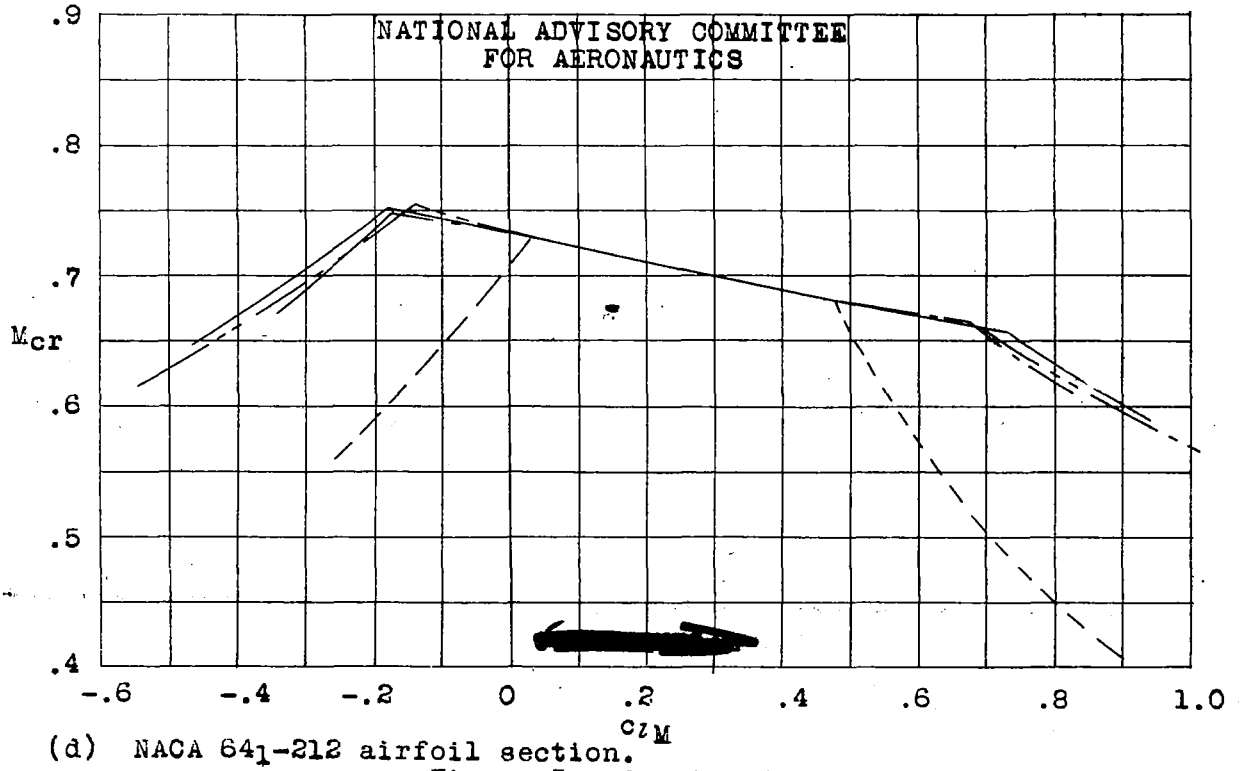

(d) NACA 64_1-212 airfoil section.
Figure 3.- Continued.

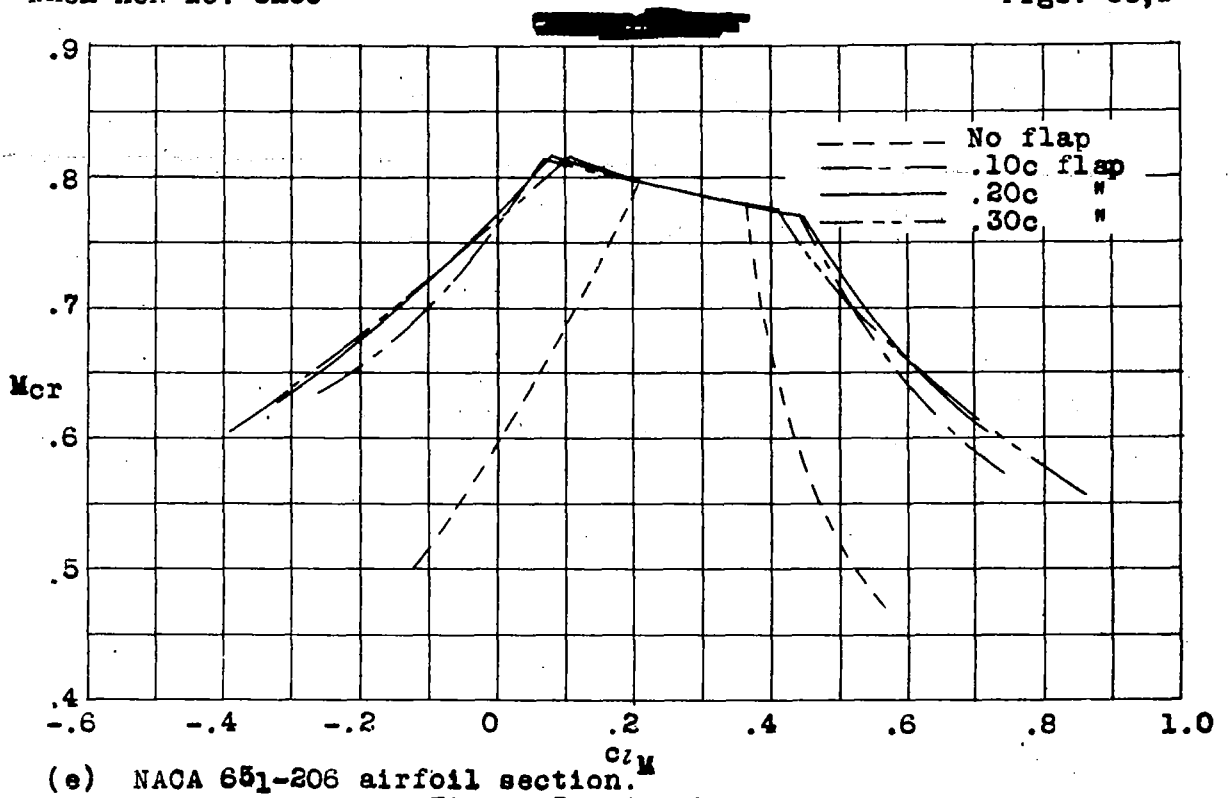

(e) NACA 65_1-206 airfoil section.

Figure 3.- Continued.

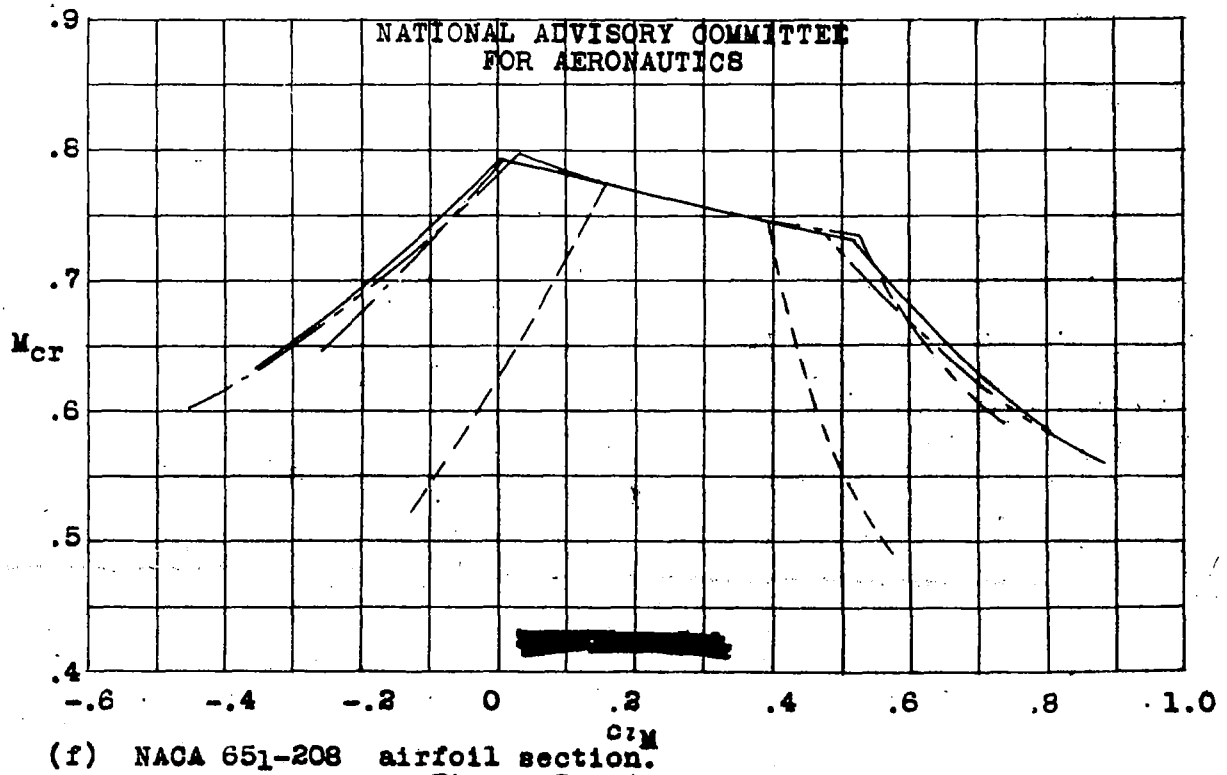

(f) NACA 65_1-208 airfoil section.

Figure 3.- Continued.

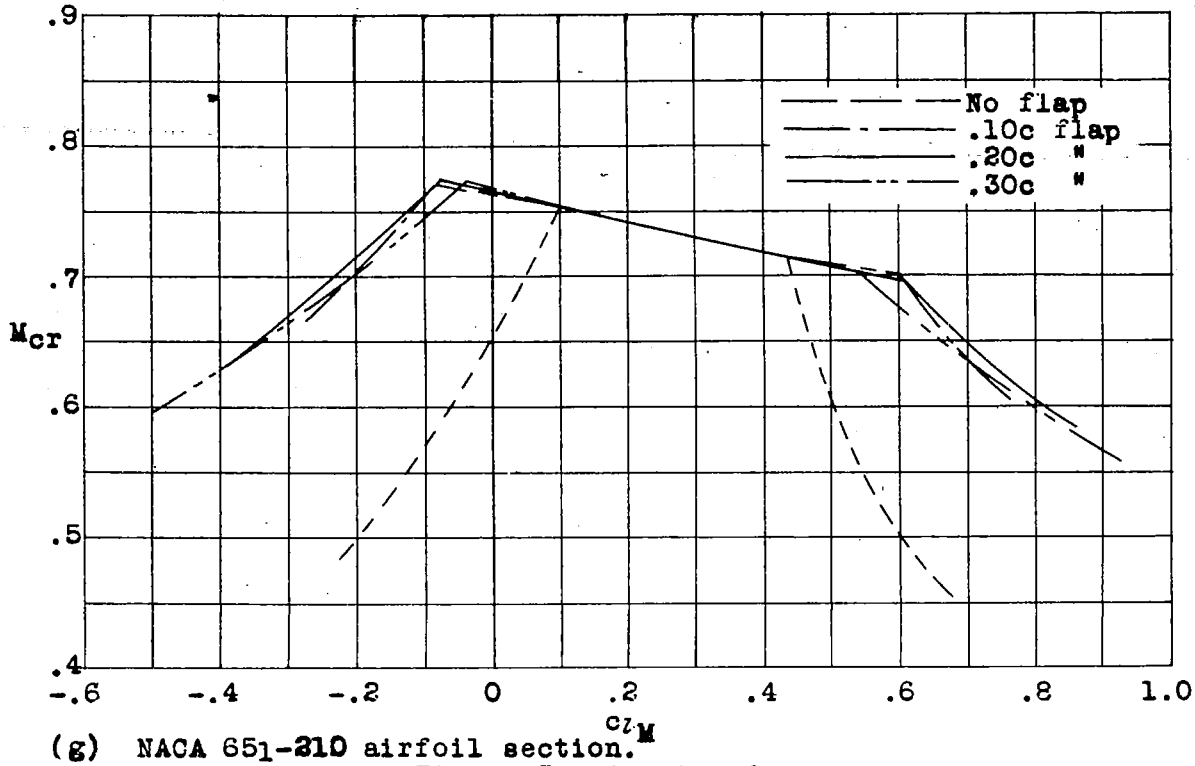

(g) NACA 65$_1$-210 airfoil section.

Figure 3.- Continued.

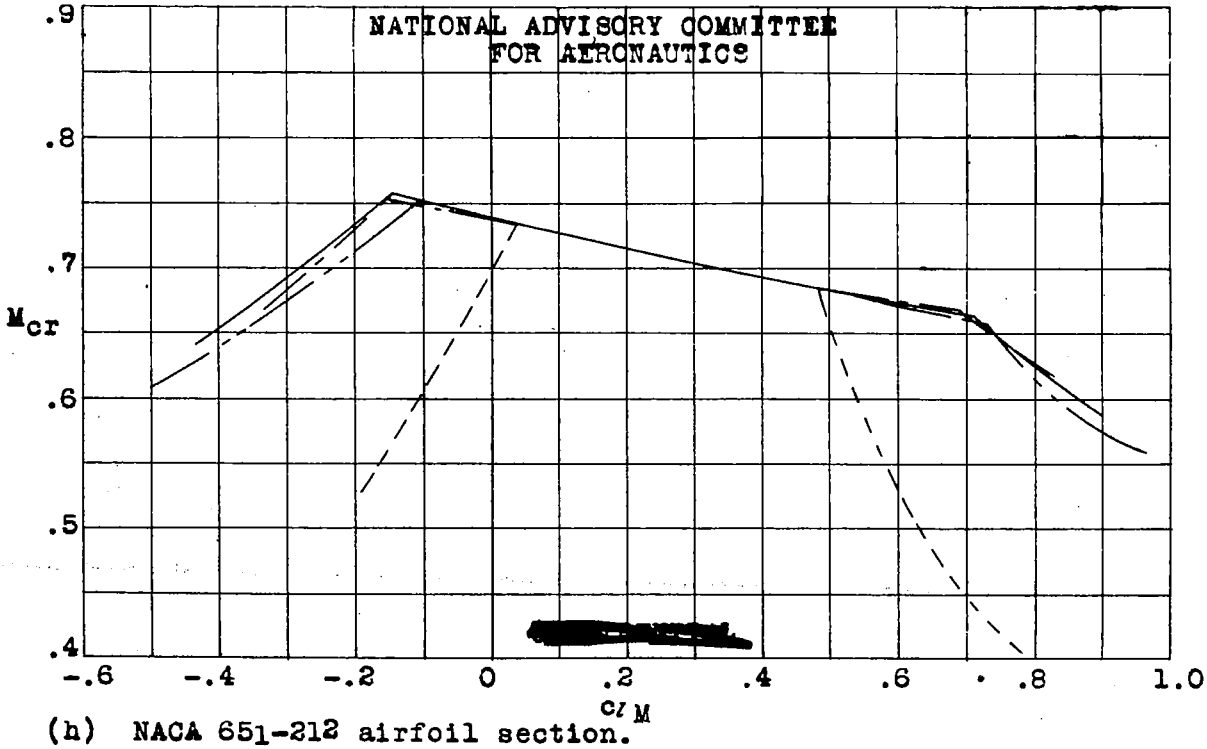

(h) NACA 65$_1$-212 airfoil section.

Figure 3.- Continued.

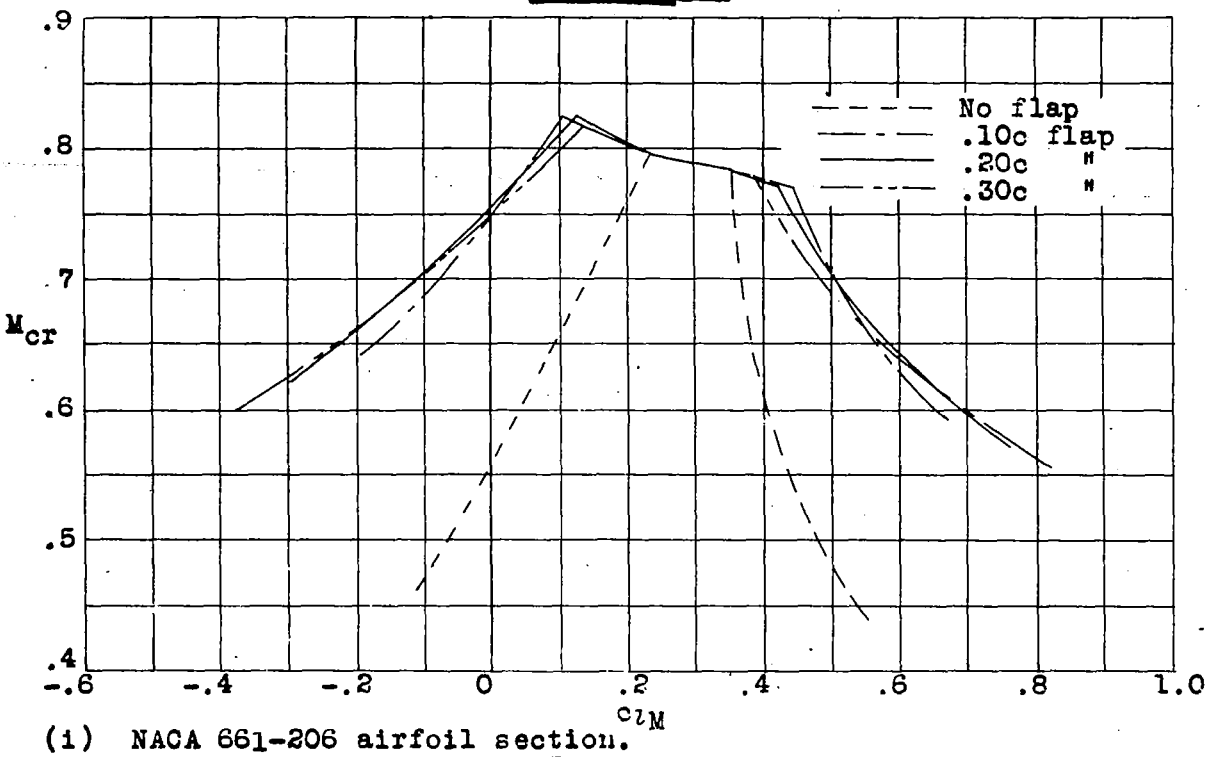

(i) NACA 661-206 airfoil section.

Figure 3.- Continued.

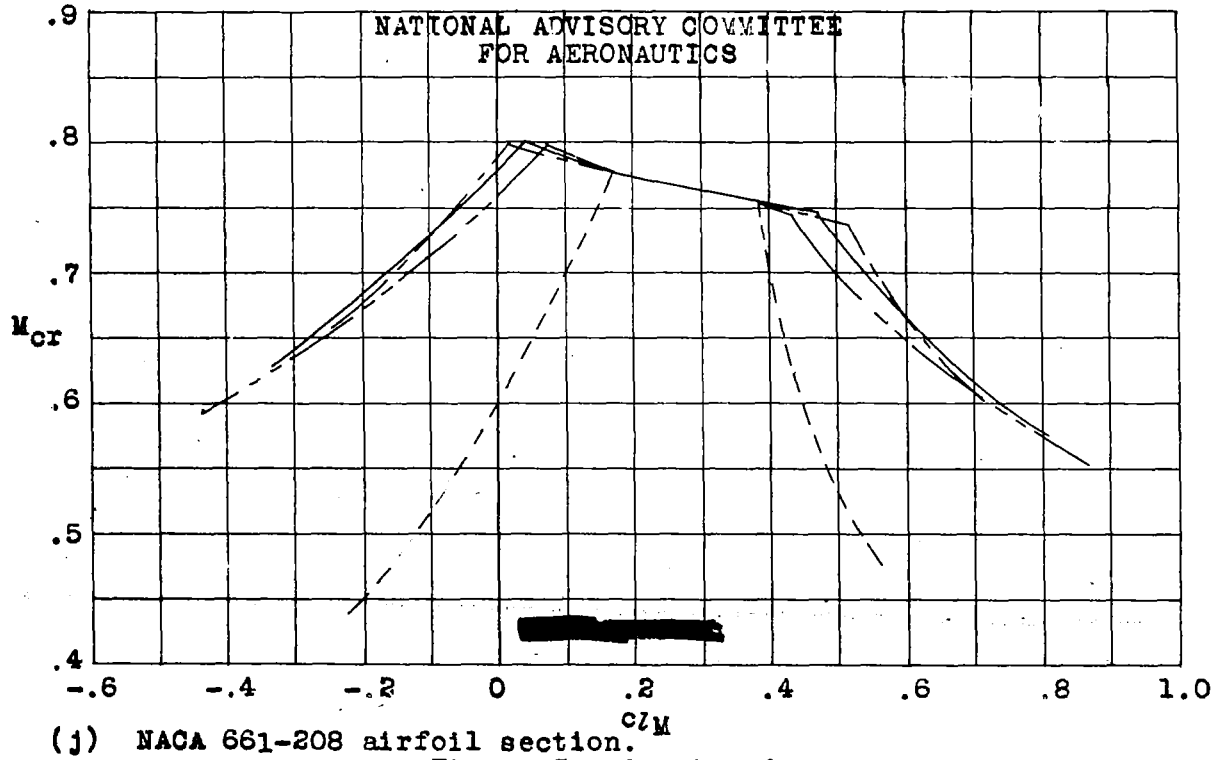

(j) NACA 661-208 airfoil section.

Figure 3.- Continued.

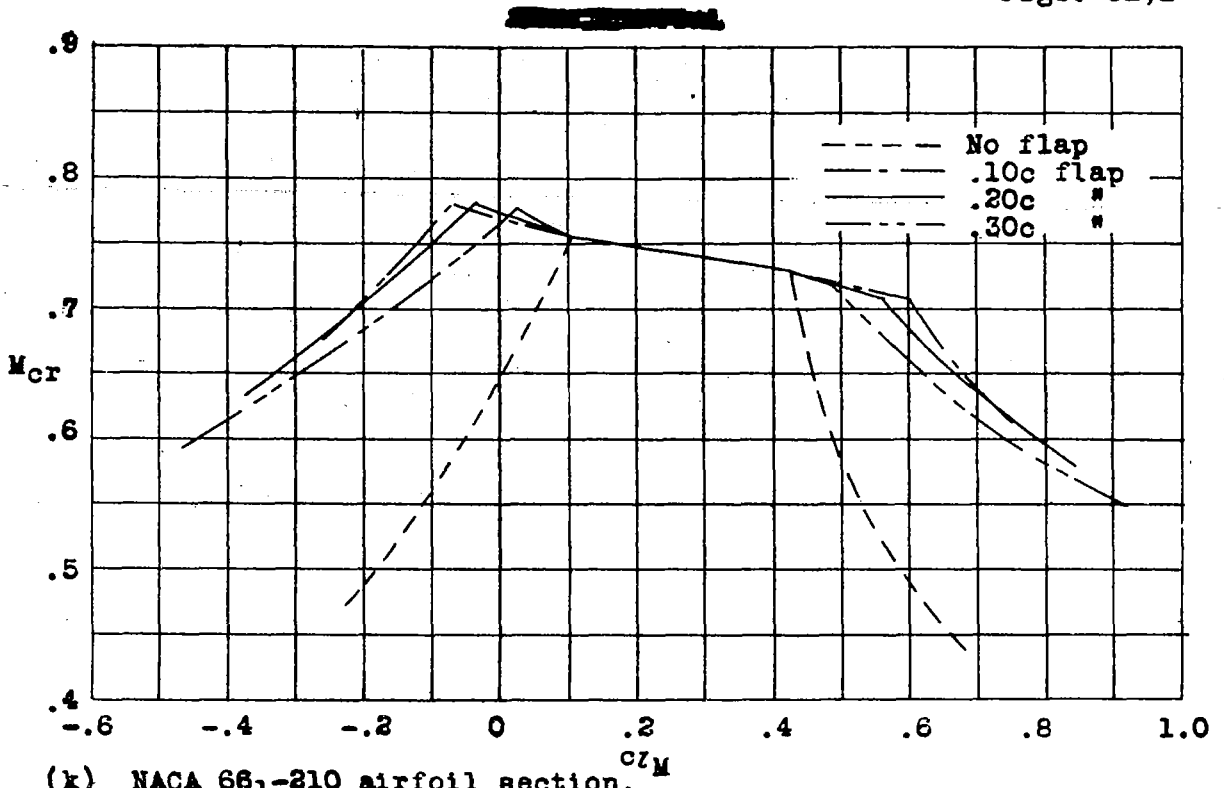

(k) NACA 66_1-210 airfoil section.

Figure 3.- Continued.

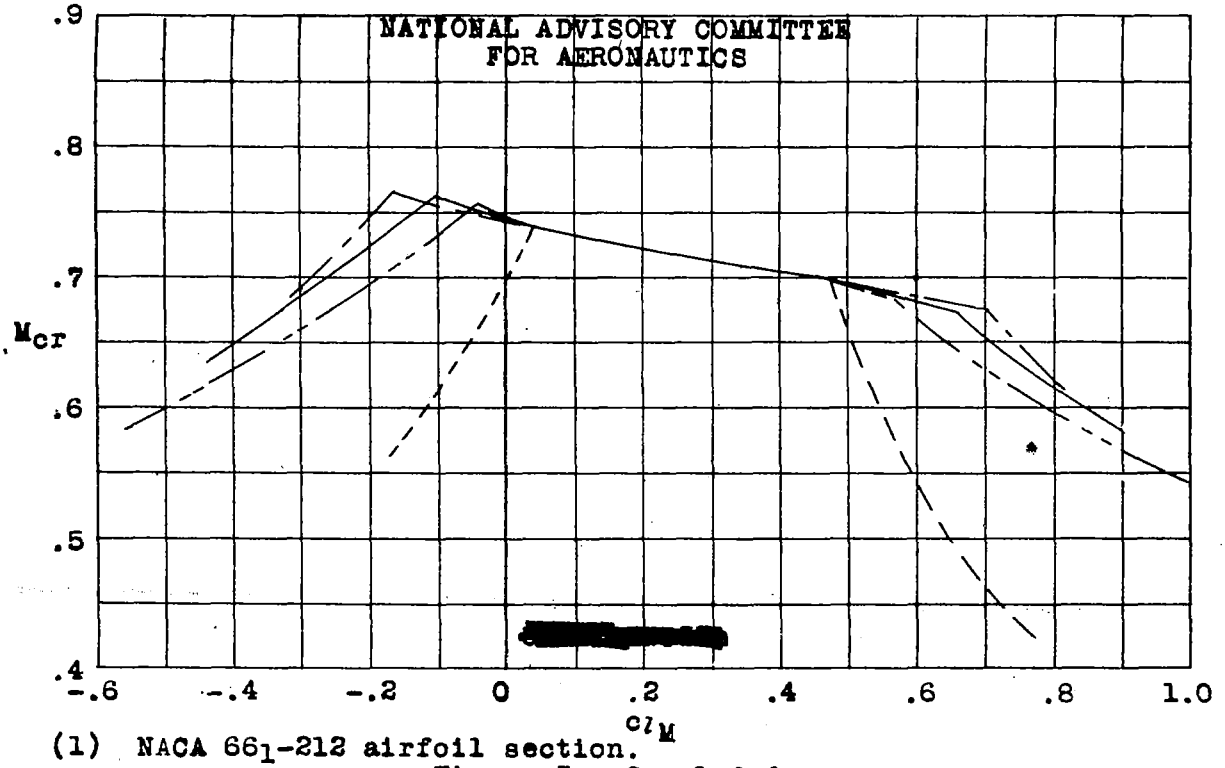

(l) NACA 66_1-212 airfoil section.

Figure 3.- Concluded.